Article:

Rockett, T.B.O., Adham, N.A., Harun, F. et al. (2 more authors) (2022) Growth of GaAsBi/GaAs multiple quantum wells with up to 120 periods. Journal of Crystal Growth, 589. 126679. ISSN 0022-0248

https://doi.org/10.1016/j.jcrysgro.2022.126679

Journal of Crystal Growth 589 (2022) 126679

Contents lists available at ScienceDirect

Journal of Crystal Growth

journal homepage: www.elsevier.com/locate/jcrysgro

Growth of GaAsBi/GaAs multiple quantum wells with up to 120 periods

Thomas B.O. Rockett [a], Nada A. Adham [a], Faezah Harun [a,b], John P.R. David [a], Robert D. Richards [a,*]

[a] *Department of Electronic and Electrical Engineering, University of Sheffield, UK*
[b] *Department of Electronics Technology, British Malaysian Institute, Universiti Kuala Lumpur, Malaysia*

ARTICLE INFO

Communicated by Maria C. Tamargo

Keywords:
A1.X-ray diffraction
A3.Molecular beam epitaxy
B1.Bismuth compounds
B2.Semiconducting III-V materials
B3.Solar cells

ABSTRACT

In this work, we demonstrate the MBE growth of a systematic series of GaAsBi/GaAs multiple quantum well devices with up to 120 periods and report on their structural and optical characterisation. TEM images confirm the incorporation of a record number of wells for this material, while showing reasonable thickness uniformity. Fitting of the XRD data becomes worse as the number of quantum wells increases due to strain relaxation and out-of-plane growth inhomogeneity. The devices are compared to a previous series of devices grown in our group using PL and are found to have less severe strain relaxation due to the thicker barriers and lower average strain in the MQW stack, despite containing a greater number of wells.

1. Introduction

GaAsBi is a promising material for multi-junction photovoltaics due to the large reduction in band gap caused by Bi incorporation into GaAs [1]. The band gap reduction per unit strain is around three times greater for Bi than for In incorporation, which is useful for multi-junction photovoltaic devices that are hindered by the lack of a 1 eV band gap material lattice matched to GaAs. Multiple quantum well (MQW) devices based on InGaAs were originally developed to ameliorate this limitation, since lattice mismatched InGaAs wells can be used to absorb lower energy photons while GaAsP barriers compensate the strain [2]. However, achieving a band gap of 1 eV using InGaAs based devices is challenging since the necessary In content is high enough that the thickness of a single well is close to the Matthews-Blakeslee critical thickness (MBCT), limiting the commercial yield and reliability. Exceeding the MBCT leads to misfit dislocations at the well interfaces which act as recombination centres. We note that InGaAs sub-cell test structures with many wells (>50) have achieved absorption edges of 1.15 eV using a complicated structure involving InGaAs step layers, GaAs interlayers, and GaAsP step layers and barriers, for aiding carrier escape and strain balancing [3]. Replacing the InGaAs layers with GaAsBi could lead to an absorption edge closer to 1 eV with a less complicated structure, a lower P content, and therefore more efficient multi-junction photovoltaics.

Previous theoretical investigations into GaAsBi have resulted in predictions of solar cell efficiencies exceeding 40% [4] and 52.5% [5]. The authors modelled 1.9 μm $GaAs0_{.95}Bi_{0.06}$ and 0.5 μm $GaAs_{0.9417}Bi_{0.0583}$ layers, respectively, in a 4-junction design. A 50 well strain compensated $GaAs_{0.965}Bi_{0.035}/GaAs_{0.75}P_{0.25}$ device was grown by MOVPE and had an efficiency of 8.25% when operated as a single junction solar cell [6]. GaAsBi MQW LEDs with 11 periods have been grown using a two-substrate temperature growth technique with a peak emission of 1.01 eV [7,8]. The absorption coefficients of GaAsBi with up to 6% Bi have been reported [9,10]. Lattice matched GaAsPBi bulk layers and MQWs with 4 periods have been grown using MBE, with the MQWs showing room temperature photoluminescence (PL) [11,12].

Our group has published studies on a series of GaAsBi / GaAs MQWs with up to 63 wells [13,14,15,16]. Research into these devices identified severe strain relaxation in devices with 54 and 63 wells, and a lower-than-expected photocurrent due to holes becoming trapped inside the wells due to the large valence band offset of GaAsBi. These devices are referred to in this work as C3-C63, with the device name denoting the number of GaAsBi wells inside the nominally 600 nm thick i-region.

A single GaAsBi well can achieve a band gap of 1 eV without exceeding the MBCT [17], therefore a GaAsBi based sub-cell is promising for multi-junction photovoltaics. Such a design could have the advantage of a simple structure compared to reference [3]; however, it is uncertain what optimisation is needed to incorporate many GaAsBi wells without undergoing strain relaxation.

In this work, we describe the MBE growth and characterisation of a

* Corresponding author.
E-mail address: R.Richards@Sheffield.ac.uk (R.D. Richards).

https://doi.org/10.1016/j.jcrysgro.2022.126679
Received 30 December 2021; Received in revised form 7 April 2022; Accepted 13 April 2022
Available online 16 April 2022

series of GaAsBi / GaAs MQWs, referred to as G2-G120, with up to 120 wells, which have a different but complementary architecture to the series discussed in references [13,14,15,16]. The devices grown in this work have varying numbers of wells with 30 nm barriers, a constant period, and different i-region thicknesses. The previous series (referred to as C3-C63) contained varying numbers of wells but different barrier thicknesses, to keep the i-region thickness constant. The new series of devices occupy a different area in the strain-thickness parameter space, with the advantage that the devices with many wells are not affected by miniband or digital alloy formation due to the thick barriers. We show that a large number of GaAsBi wells can be incorporated into GaAs by reducing the average strain per period of the MQW stack. We show PL and x-ray diffraction (XRD) measurements that highlight the reduced strain relaxation that is possible when using thicker barriers, despite the large numbers of wells (up to 120) that are incorporated.

2. Experimental methods

MBE growth was performed in an Omicron MBE-STM on GaAs (0 0 1) 0.1° off cut substrates. Solid source effusion cells were used for Ga, Bi, Si, and Be, while a valved cracker effusion cell was used to produce As_2 and As_4. Growth temperatures quoted in this work were calibrated using RHEED transitions and have a precision of ± 3 °C, however the uncertainty is approximately ± 10 °C. A Bruker D8 Discover was used to measure (0 0 4) ω-2θ scans and RADS Mercury was used to fit the data. Transmission electron microscopy (TEM) images were gathered using a Jeol 2000FX TEM. PL measurements were performed with a 532 nm laser (300 mW, estimated power density 120 W/cm^2), an LN_2 cooled Ge detector, phase sensitive detection, and a monochromator.

2.1. Growth

The GaAsBi/GaAs MQWs were grown inside the i-region of a p-i-n diode structure, see Fig. 1. The GaAsBi wells and GaAs barriers were grown at a rate of 0.59 monolayer/s at 375 °C using As_4 [18] and an As:Ga atomic flux ratio of 1.8:1. Due to the incorporation dynamics of As_4 only half of the As atoms can incorporate, resulting in a small As flux deficit and Ga rich growth. However, a Ga rich RHEED reconstruction was not observed since the wells and barriers are thin, the As flux deficit is small, and 30 (60) second growth pauses were used after each well (barrier) was deposited to anneal the surface at the growth temperature of 375 °C [19].

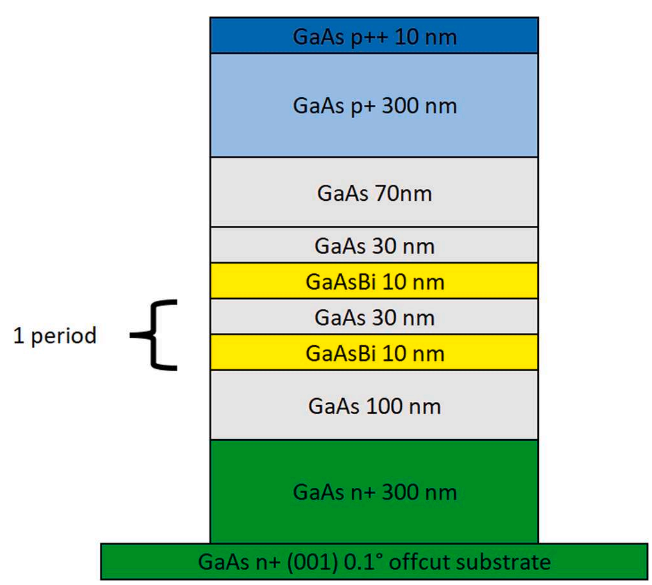

Fig. 1. Device structure of G2 (2 periods). The GaAsBi 10 nm / GaAs 30 nm period is repeated up to 120 times in the other devices.

The Bi beam equivalent pressure was 1.1 × 10^{-7} mBar as measured using an ion gauge in front of the substrate. A Bi wetting layer was built up by opening the shutter for 30 s prior to the growth of the first quantum well [20]. The RHEED pattern changed from As terminated c (4 × 4) to a Bi terminated (n × 3) reconstruction [21].

The GaAs layers were grown at 577 °C using As_2 with an As:Ga atomic flux ratio of 1.5:1. The Be and Si doping in the 300 nm thick p and n-type GaAs layers was 3 × 10^{18} and 2 × 10^{18} cm^{-3}, respectively. The 100 nm thick GaAs cladding layers were used to prevent dopant atoms from diffusing into the MQW stack. The i-region of each device was annealed during the growth of the upper GaAs layers for around 1 h, including the time taken to change the As cracker temperature to produce As_2. A list of the devices grown in this work is shown in Table 1.

The average strain [22] is plotted against the MQW stack thickness in Fig. 2, for the devices grown in this work (series G) and the previous Sheffield grown MQWs (series C). The new devices allow the investigation of the critical thickness in a different part of the parameter space.

An example schematic band structure for device G2 under zero bias is shown in Fig. 3. From Fig. 3 one would expect the electrons are more loosely bound inside the wells, which has implications for the carrier collection efficiency.

2.2. XRd

XRD spectra are shown in Fig. 4. The MQW periods are comparable since satellite peaks are visible at similar angles in all the devices. Interference fringes are not visible for 15+ wells, corresponding roughly to the point where the MQW stack thickness exceeds the MBCT. The satellite peaks become broader as the number of wells increases due to strain relaxation and compositional inhomogeneity building up out-of-plane during the growth leading to a gradual reduction in the quality of the fitting.

2.3. TEm

Representative TEM images of G120 are shown in Fig. 5. The wells are easily identifiable in Fig. 5(a). Many defects are visible in well 109 near the top of the stack, which corresponds closely to the estimated Drigo critical thickness. However, it is unlikely that such a sharp distribution of defects is related to the critical thickness, and this is probably a coincidence. The defects may be dislocation loops or Bi inclusions, caused by non-optimal growth conditions or high dopant levels.

Fig. 5(b) shows a close-up of the defects and displays the uniformity of the well interfaces. The TEM measurements show that all the wells are 7 ± 0.5 nm, except for the first well in the stack which was around 1 nm thicker, likely due to the Bi wetting layer.

2.4. Photoluminescence

PL measurements of selected devices are shown in Fig. 6, including previous devices grown in Sheffield for comparison. From Fig. 6, the

Table 1
List of GaAsBi/GaAs MQW devices grown in this work. The Bi content and layer thicknesses extracted from XRD simulations are shown, along with the magnitude of the average strain in the MQW stack |f|. The number in the device name corresponds to the number of wells in that device.

Device name	Bi content (%)	Well thickness (nm)	Barrier thickness (nm)	|f| (%)
G2	4.3	8	32.5	0.156
G5	4.5	6.6	30.9	0.105
G15	5.1	6.1	32.5	0.094
G40	5.2	5.7	31.1	0.091
G80	5.5	5.4	32	0.087
G120	5.5	5.4	31.2	0.091

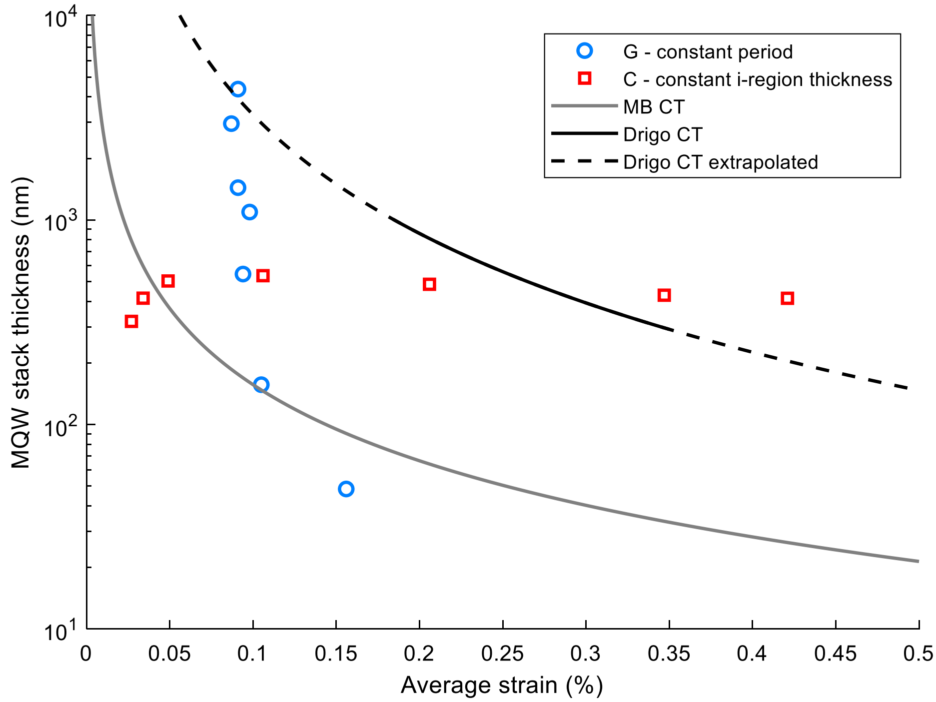

Fig. 2. Average strain in the GaAsBi/GaAs MQW stack plotted against the stack thickness. The Matthews-Blakeslee and Drigo critical thicknesses are also plotted and correspond to the point at which the strain energy is high enough for dislocations to become mobile [23] or for the formation of new dislocations, respectively. The Drigo critical thickness [24] is based on an empirical fit to data published in reference [22], and the dashed black line is extrapolated.

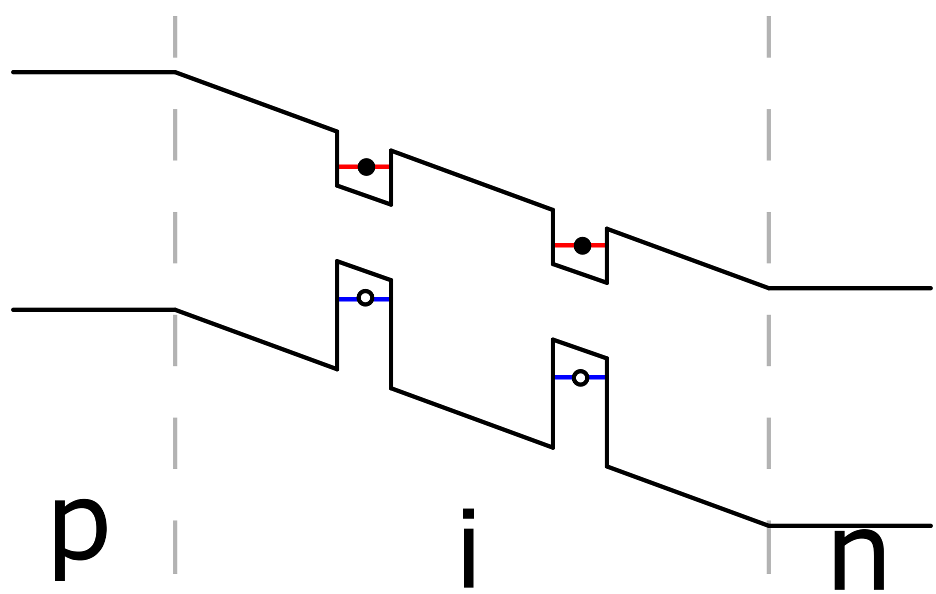

Fig. 3. Example schematic diagram of device G2 under zero bias, consisting of two GaAsBi quantum wells inside a GaAs p-i-n diode.

GaAsBi devices show PL peaks in the range 1.16–1.18 eV, with FWHM values around 75 meV. The exceptions are C53 and C64, which are red shifted to 1.11 and 1.12 eV, respectively, due to a combination of strain relaxation and/or a loss of carrier confinement as discussed in reference [14]. The series G devices show a prominent GaAs peak at 1.42 eV which originates from the GaAs capping layer.

Since the two sets of MQWs have different periods and are in different parts of the strain/thickness parameter space, comparing their integrated PL intensity (IPL) based on the number of wells is not a fair comparison. The product of the average strain in the MQW stack and the stack thickness was used instead, see Fig. 7.

From Fig. 7, the IPL is roughly linearly proportional to the strain-thickness product up to around 130 %nm. The GaAsBi is expected to have many non-radiative recombination centres due to the low growth temperature, which should lead to a super-linear relationship between IPL and carrier density and therefore a decrease in IPL as the number of wells increases due to the number of carriers per well decreasing as more wells are incorporated. However, the laser power may be high enough to ensure the carrier density is sufficiently high enough to saturate the non-radiative defects in the wells, at least in the devices with fewer wells. The high laser power may also lead to the ground state of the wells being fully occupied with carriers, causing the IPL to be proportional to the volume of GaAsBi available for recombination, i.e., proportional to the number of wells. We note that there is no obvious high energy shoulder

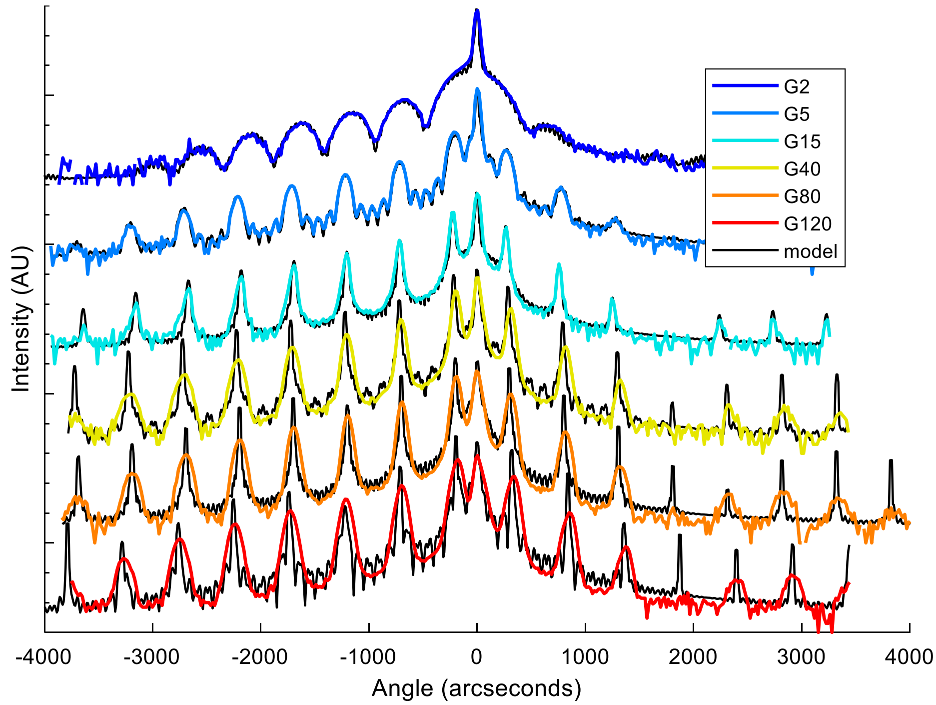

Fig. 4. XRD (0 0 4) ω-2θ scans of the GaAsBi/GaAs MQWs grown in this work.

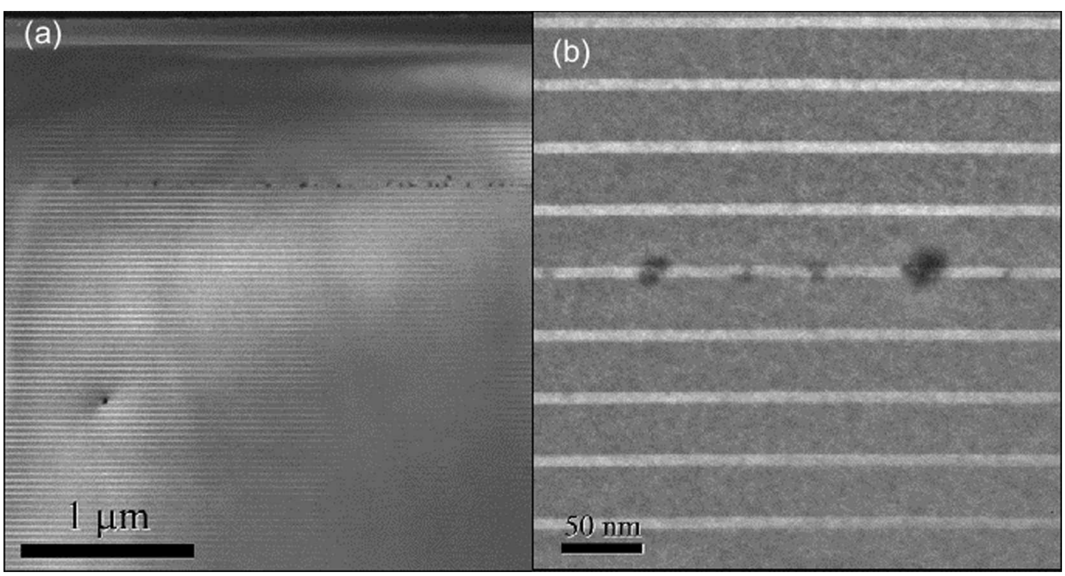

Fig. 5. Dark field TEM images of G120; (a) 5 k magnification, (b) 50 k magnification focussing on well 109.

on the main peaks in Fig. 6: the absence of any higher order transitions is likely caused by the low conduction band offset in the wells.

Above 130 %nm there is a rapid decrease in IPL for series C (constant stack thickness) and a slower decrease for series G (constant period). The rapid decrease for series C is caused by strain relaxation and a loss of carrier confinement, as discussed previously.

There are several mechanisms that contribute to the decrease in IPL exhibited by series G. Firstly, there is some additional strain relaxation in G80 and G120 relative to G40. These devices are much thicker than the MBCT for dislocation mobilisation, so threading dislocations can move into the interface planes at the top and bottom of the MQW stack and become misfit dislocations leading to enhanced non-radiative recombination of carriers at the MQW interfaces. Secondly, as previously discussed, the number of carriers per well is reduced in the devices with more wells, so the defects may not be saturated and will instead lead to most of the carriers recombining non-radiatively. Thirdly, photons reabsorption by wells closer to the surface of the devices will limit the IPL of the thicker devices. The roughly 35x greater IPL of G80 and G120 compared to C54 and C63, despite the considerably larger number of wells and greater overall strain, shows the benefit of the lower average strain in the MQW stack caused by the thicker barriers.

The incorporation of up to 120 GaAsBi wells into a test structure without any strain compensation is promising for multi-junction photovoltaics and shows clear advantages over InGaAs. This could lead to future test structures with more complicated structures. However, the use of thicker barriers reduces the built-in electric field and will result in a lower carrier collection efficiency. There is therefore a trade-off between the number of quantum wells that can be incorporated, and hence

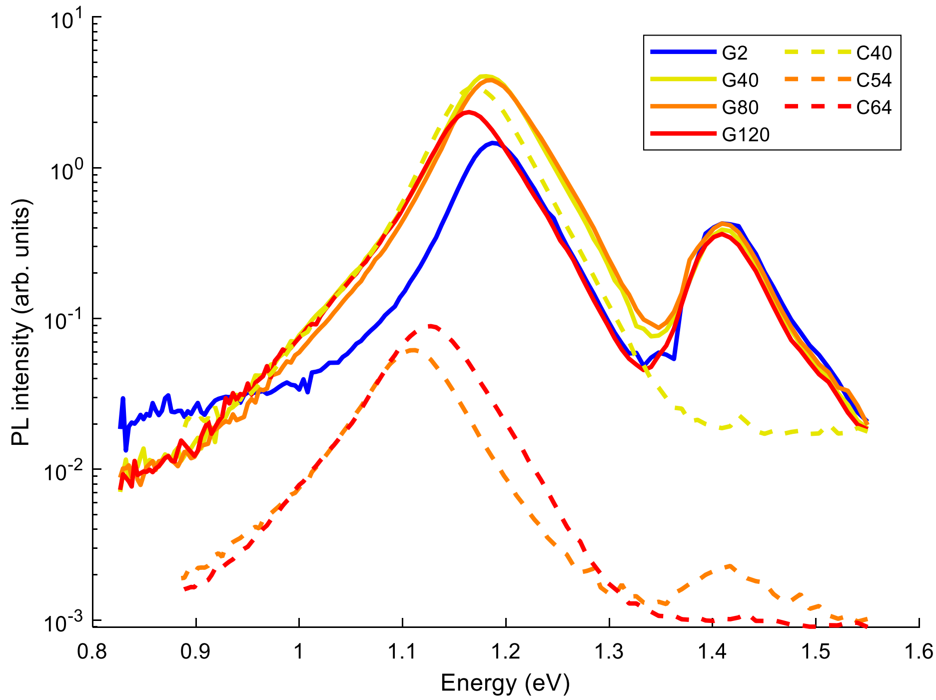

Fig. 6. Photoluminescence spectra of selected GaAsBi/GaAs MQWs. The solid and dashed lines represent MQWs with a constant period and constant stack thickness, respectively.

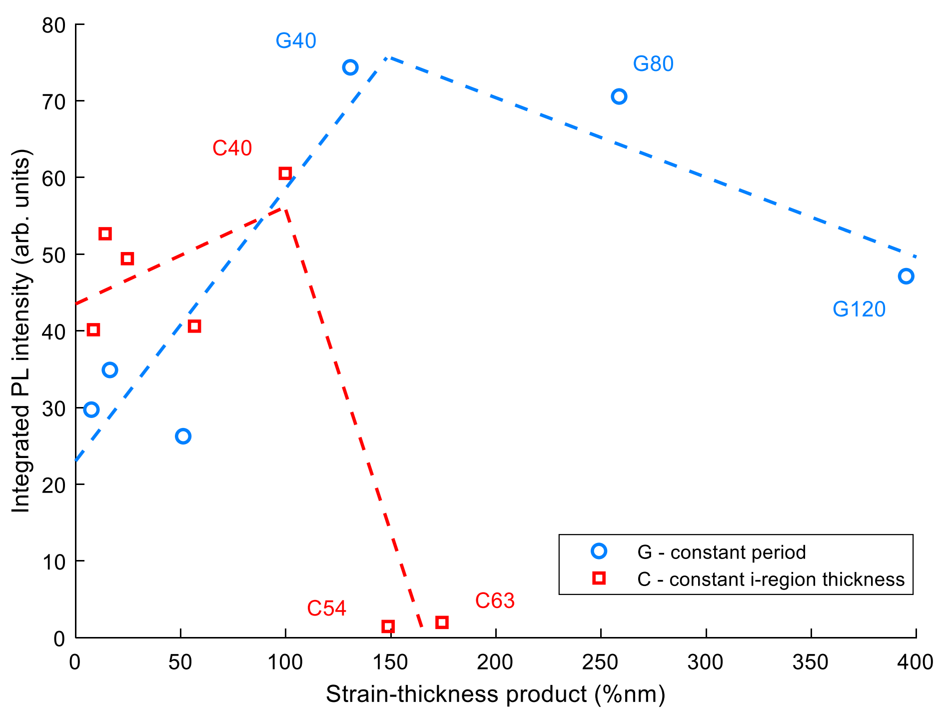

Fig. 7. Integrated PL of GaAsBi/GaAs MQWs under 120 W/cm^2 excitation at 532 nm as a function of the strain-thickness product of the MQW stack. The lines are drawn to guide the eye. Several of the devices are labelled for clarity.

the light absorption, and the carrier collection efficiency since the built-in electric field is dependent on the depletion region thickness. Reducing the ground state transition energy from the 1.16–1.18 eV shown in this work to the optimal 1 eV is challenging due to the growth difficulty of incorporating the required Bi content (~7%), however researchers have shown PL with up to 10.8% Bi [17]. Although GaAsBi suffers from larger linewidths than InGaAs due to the localised states in the valence band, we note that dilute nitride GaAsN devices also suffer from large linewidths due to localised states in the conduction band [25]. Dilute nitride containing layers have been present in several world record solar cell devices in recent years [26,27], so the large spectral broadening of GaAsBi will likely not prohibit it from proving useful for future photovoltaic devices. The radiative efficiency in GaAsBi is also lower than InGaAs, however our previous studies have indicated a moderate ~ 15x reduction in IPL between GaAsBi/GaAs 40 MQW and a strain-compensated InGaAs/GaAsP 65 MQW [28].

We propose that future GaAsBi based photovoltaic research could focus on comparing GaAsBi/GaAs/GaAsP strain balanced quantum wells with strain balanced bulk GaAsBiN. The growth of GaAsBiN devices is challenging due to the growth difficulty of incorporating both Bi and N [29,30,31,32], and the deleterious effect of the N on the electron mobility [33]. Meanwhile, GaAsBi / GaAs / GaAsP devices will require careful optimisation for efficient carrier collection, and the structure design may follow similar principles established for InGaAs / GaAs / GaAsP devices [34,35,36], with graded InGaAs layers to aid carrier escape and strain compensation via either thin GaAsP barriers (escape via tunnelling) or thicker GaAsP barriers with a lower P content (thermal escape).

3. Conclusion

We demonstrate the MBE growth of GaAsBi/GaAs multiple quantum well photovoltaic test structures with up to 120 periods. TEM measurements highlight the relatively uniform periodicity and composition of the wells. However, XRD measurements show a gradual decrease in the accuracy of the fitting as the number of wells increases due to some strain relaxation and out-of-plane growth inhomogeneity. PL measurements confirm that the 120 well device shows less severe strain relaxation than a previous 63 well device grown in our group. This is attributed to the thicker barriers and lower average strain in the MQW stack, despite the greatly increased number of quantum wells. These results should prove useful for the design of future strain-compensated GaAsBi/GaAs/GaAsP multiple quantum well structures, although significant optimisation is needed to produce a competitive device.

CRediT authorship contribution statement

Thomas B.O. Rockett: Conceptualization, Methodology, Software, Formal analysis, Investigation, Data curation, Writing – original draft, Visualization. **Nada A. Adham:** Investigation, Data curation. **Faezah Harun:** Investigation, Data curation. **John P.R. David:** Conceptualization, Writing – review & editing. **Robert D. Richards:** Conceptualization, Writing – review & editing, Supervision, Funding acquisition.

Declaration of Competing Interest

The authors declare that they have no known competing financial interests or personal relationships that could have appeared to influence the work reported in this paper.

Acknowledgements

The authors would like to thank Richard Beanland for TEM measurements. The work of RDR was part-funded by the Royal Academy of Engineering through the research fellowships scheme (RF1516\15\43). The work of TBOR and RDR was part-funded by EPSRC (EP/S036792/1).

References

[1] K. Alberi, O.D. Dubon, Valence band anticrossing in GaBixAs1-x, Appl. Phys. Lett. 91 (2007), 051909.
[2] N.J. Ekins-Daukes, K.W.J. Barnham, J.P. Connolly, J.S. Roberts, J.C. Clark, G. Hill, M. Mazzer, Strain-balanced GaAsP/InGaAs quantum well solar cells, Appl. Phys. Lett. 75 (26) (1999) 4195–4197.
[3] K. Toprasertpong, H. Fujii, T. Thomas, M. Führer, D. Alonso-Álvarez, D.J. Farrell, K. Watanabe, Y. Okada, N.J. Ekins-Daukes, M. Sugiyama, Y. Nakano, Absorption threshold extended to 1.15 eV using InGaAs/GaAsP quantum wells for over-50%-efficient lattice-matched quad-junction solar cells, Prog. Photovolt: Res. Appl. 24 (4) (2016) 533–542.
[4] T. Thomas, A. Mellor, N.P. Hylton, M. Führer, D. Alonso-Álvarez, A. Braun, N. J. Ekins-Daukes, J.P.R. David, S.J. Sweeney, Requirements for a GaAsBi 1 eV sub-cell in a GaAs-based multi-junction solar cell, Semicond. Sci. Technol. 30 (2015), 094010.
[5] S. Khanom, M. K. Hossain, F. Ahmed, M. A. Hossain, A. Kowsar and M. Rahaman, Simulation study of multijunction solar cell incorporating GaAsBi, in 2017 IEEE Region 10 Humanitarian Technology Conference, Dhaka, Bangladesh, 2017.
[6] H. Kim, K. Kim, Y. Guan, J. Lee, T.F. Kuech, L.J. Mawst, Single junction solar cell employing strain compensated GaAs0.965Bi0.035/GaAs0.75P0.25 multiple quantum wells grown by metal organic vapor phase epitaxy, Appl. Phys. Lett. 112 (2018), 251105.
[7] P.K. Patil, E. Luna, T. Matsuda, K. Yamada, K. Kamiya, F. Ishikawa, S. Shimomura, GaAsBi/GaAs multi-quantum well LED grown by molecular beam epitaxy using a two-substrate-temperature technique, Nanotechnology 28 (10) (2017), 105702.
[8] P.K. Patil, F. Ishikawa, S. Shimomura, GaAsBi/GaAs MQWs grown by MBE using a two-substrate-temperature technique, J. Alloy. Compd. 725 (2017) 694–699.
[9] C.J. Hunter, F. Bastiman, A.R. Mohmad, R.D. Richards, J.S. Ng, S.J. Sweeney, J.P. R. David, Absorption Characteristics of GaAs1-xBix/GaAs Diodes in the Near-Infrared, IEEE Photonics Technol. Lett. 24 (23) (2012) 2191–2194.
[10] Z. Zhou, D.F. Mendes, R.D. Richards, F. Bastiman, J.P.R. David, Absorption properties of GaAsBi based p–i–n heterojunction diodes, Semicond. Sci. Technol. 30 (9) (2015), 094004.
[11] C. Himwas, S. Kijamnajsuk, V. Yordsri, C. Thanachayanont, T. Wongpinij, C. Euaruksakul, S. Panyakeow, S. Kanjanachuchai, Optical properties of lattice-matched GaAsPBi multiple quantum wells grown on GaAs (001), Semicond. Sci. Technol. 36 (4) (2021), 045014.
[12] C. Himwas, A. Soison, S. Kijamnajsuk, T. Wongpinij, C. Euaraksakul, S. Panyakeow, S. Kanjanachuchai, GaAsPBi epitaxial layer grown by molecular beam epitaxy, Semicond. Sci. Technol. 35 (9) (2020), 095009.
[13] R.D. Richards, F. Bastiman, D. Walker, R. Beanland, J.P.R. David, Growth and structural characterization of GaAsBi/GaAs multiple quantum wells, Semicond. Sci. Technol. 30 (9) (2015), 094013.
[14] R.D. Richards, F. Bastiman, J.S. Roberts, R. Beanland, D. Walker, J.P.R. David, MBE grown GaAsBi/GaAs multiple quantum well structures: Structural and optical characterization, J. Cryst. Growth 425 (2015) 237–240.
[15] R.D. Richards, A. Mellor, F. Harun, J.S. Cheong, N.P. Hylton, T. Wilson, T. Thomas, J.S. Roberts, N.J. Ekins-Daukes, J.P.R. David, Photovoltaic characterisation of GaAsBi/GaAs multiple quantum well devices, Sol. Energy Mater. Sol. Cells 172 (2017) 238–243.
[16] R.D. Richards, T.B.O. Rockett, M.R.M. Nawawi, F. Harun, A. Mellor, T. Wilson, C. Christou, S. Chen, J.P.R. David, Light-biased IV characteristics of a GaAsBi/GaAs multiple quantum well pin diode at low temperature, Semicond. Sci. Technol. 33 (2018), 094008.
[17] A.R. Mohmad, F. Bastiman, C.J. Hunter, R.D. Richards, S.J. Sweeney, J.S. Ng, J.P. R. David, B.Y. Majlis, Localization effects and band gap of GaAsBi alloys, Physica Status Solidi (b) 251 (6) (2014) 1276–1281.
[18] R.D. Richards, F. Bastiman, C.J. Hunter, D.F. Mendes, A.R. Mohmad, J.S. Roberts, J.P.R. David, Molecular beam epitaxy growth of GaAsBi using As2 and As4, J. Cryst. Growth 390 (2014) 120–124.
[19] E. O. Göbel, K. Ploog, Fabrication and optical properties of semiconductor quantum wells and superlattices, Prog. Quantum Electron. 14 (4) (1990) 289–356.
[20] R. B. Lewis, M. Masnadi-Shirazi and T. Tiedje, Growth of high Bi concentration GaAs1-xBix by molecular beam epitaxy, Applied Physics Letters, vol. 101, no. 082112, 2012.
[21] F. Bastiman, A.G. Cullis, J.P.R. David, S.J. Sweeney, Bi incorporation in GaAs(100)-2×1 and 4×3 reconstructions investigated by RHEED and STM, J. Cryst. Growth 341 (1) (2012) 19–23.
[22] P.R. Griffin, J. Barnes, K.W.J. Barnham, G. Haarpaintner, M. Mazzer, C. Zanotti-Fregonara, E. Grünbaum, C. Olson, C. Rohr, J.P.R. David, J.S. Roberts, R. Grey, M. A. Pate, Effect of strain relaxation on forward bias dark currents in GaAs/InGaAs multiquantum well p–i–n diodes, J. Appl. Phys. 80 (10) (1996) 5815–5820.
[23] S.M. Hu, Misfit dislocations and critical thickness of heteroepitaxy, J. Appl. Phys. 69 (11) (1991) 7901–7903.
[24] A.V. Drigo, A. Aydinli, A. Carnera, F. Genova, C. Rigo, C. Ferrari, P. Franzosi, G. Salviati, On the mechanisms of strain release in molecular-beam-epitaxy-grown InxGa1−xAs/GaAs single heterostructures, J. Appl. Phys. 66 (5) (1989) 1975–1983.
[25] W. Dawidowski, B. Ściana, M. Latkowska, D. Radziewicz, D. Pucicki, K. Bielak, M. Badura and M. Tłaczała, Influence of rapid thermal annealing on optical properties of (In, Ga)(As, N)/GaAs quantum wells, in Proceedings of SPIE - The International Society for Optical Engineering, Ryn, Poland, 2013.
[26] M. Wiemer, V. Sabnis and H. Yuen, 43.5% efficient lattice matched solar cells, in Proceedings of SPIE - The International Society for Optical Engineering, San Diego, USA, 2011.
[27] R. Jones-Albertus, E. Becker, R. Bergner, T. Bilir, D. Derkacs, O. Fidaner, D. Jory, T. Liu, E. Lucow, P. Misra, E. Pickett, F. Suarez, A. Sukiasyan, T. Sun, L. Zhang, V. Sabnis, M. Wiemer, H. Yuen, Using dilute nitrides to achieve record solar cell efficiencies, Materials Research Society Symposium 1528 (2013) 161–166.
[28] R. D. Richards, Bastiman, H. C. J. F., A. R. Mohmad, J. P. R. David and N. Ekins-Daukes, GaAsBi MQWs for multi-junction photovoltaics, in IEEE 39th Photovoltaics Specialists Conference, Tampa, Florida, USA, 2013.
[29] E.-M. Pavelescu, O. Ligor, J. Occena, C. Ticoş, A. Matei, R.L. Gavrilă, K. Yamane, A. Wakahara, R.S. Goldman, Influence of electron irradiation and rapid thermal annealing on photoluminescence from GaAsNBi alloys, Appl. Phys. Lett. 117 (2020), 142106.
[30] J. Occena, T. Jen, E.E. Rizzi, T.M. Johnson, J. Horwath, Y.Q. Wang, R.S. Goldman, Bi-enhanced N incorporation in GaAsNBi, Appl. Phys. Lett. 110 (2017), 242102.
[31] J. Occena, T. Jen, H. Lu, B.A. Carter, T.S. Jimson, A.G. Norman, R.S. Goldman, Surfactant-induced chemical ordering of GaAsN: Bi, Appl. Phys. Lett. 113 (21) (2019), 211602.

[32] H. Kawata, S. Hasegawa, J. Matsumura, H. Nishinaka, M. Yoshimoto, Fabrication of a GaAs/GaNAsBi solar cell and its performance improvement by thermal annealing, Semicond. Sci. Technol. 36 (2021), 095020.

[33] M. Inagaki, S. Kimura, K. Ikeda, N. Kohima, Y. Ohshita and M. Yamaguchi, Effect of N-induced scattering centers on electron mobility in CBE grown GaAsN films, in 37th IEEE Photovoltaic Specialists Conference, Seattle, WA, USA, 2011.

[34] H. Fujii, K. Watanabe, M. Sugiyama, Y. Nakano, Effect of Quantum Well on the Efficiency of Carrier Collection in InGaAs/GaAsP Multiple Quantum Well Solar Cells, Jpn. J. Appl. Phys. 51 (10S) (2012) 10ND04, https://doi.org/10.7567/JJAP.51.10ND04.

[35] H. Fujii, K. Toprasertpong, K. Watanabe, M. Sugiyama, Y. Nakano, Evaluation of Carrier Collection Efficiency in Multiple Quantum Well Solar Cells, IEEE J. Photovoltaics 4 (1) (2014) 237–243.

[36] Y. Yazawa, T. Kitatani, J. Minemura, K. Tamura and T. Warabisako, Carrier generation and transport in InGaAs/GaAs multiple quantum well solar cells, in IEEE 1st World Conference on Photovoltaic Energy Conversion - WCPEC, Waikoloa, HI, USA, 1994.